An infrared evanescent wave sensor for detection of ascorbic acid in food and drugs

Tianxiang You, Yongkun Zhao, Yantao Xu, Haitao Guo, Jihong Zhu, Haizheng Tao, Xianghua Zhang, Yinsheng Xu

JLT-33135-2023

An infrared evanescent wave sensor for detection of ascorbic acid in food and drugs

Tianxiang You, Yongkun Zhao, Yantao Xu, Haitao Guo, Jihong Zhu, Haizheng Tao, Xianghua Zhang, and Yinsheng Xu

***Abstract*—An infrared evanescent wave sensor was developed to accurately detect ascorbic acid (vitamin C) in food and drugs. The sensor was fabricated by tapering and bending of As_2S_3 infrared fibers. Due to the broad transmission range (5000-1500 cm^{-1}) of the infrared fibers, covering the characteristic absorption peak of ascorbic acid (C=O at 1760 cm^{-1} and C=C at 1690 cm^{-1}), the sensor is capable of accurately identifying and detecting the concentration of ascorbic acid. Experimental results demonstrated that a conically tapered fiber sensor with a waist diameter of 50 μm, waist length of 30 mm, and a radius of 2 mm achieved a maximum sensitivity of 0.1257 (a.u./(mg·ml^{-1})) and a limit of detection (LoD) of 0.917 mg/ml. Furthermore, the application of this fiber sensor in various vitamin C-containing tablets and juices validated its high accuracy and minimal measurement deviation (as low as 0.19 mg/ml). Compared to traditional detection methods, the sensor not only provides a faster and cost-effective solution to identify the substance but also maintains high accuracy. It offers a new approach to quantitative and qualitative analysis of food and drugs.**

***Index Terms*—ring fiber sensor, tapered fiber, infrared fiber, ascorbic acid detection, evanescent wave**

I. INTRODUCTION

Food and drug safety, as well as quality regulation, are global issues that not only concern the protection of consumer rights but also directly impact human health. Ascorbic acid ($C_6H_8O_6$), an essential nutrient for the human body, plays a crucial role in preventing and mitigating many chronic diseases, such as heart disease and cancer[1],[2]. To maintain good health and prevent disease, people often rely on supplements or medications that are fortified with ascorbic acid. It is worth noting that while ascorbic acid is a safe nutrient, excessive intake can negatively affect the body[3]. However, the quality of ascorbic acid products in the market varies, and there have been cases of fake products with low ascorbic acid content[4]. Therefore, it is necessary to develop a cost-effective and convenient technique that can accurately identify and detect ascorbic acid to ensure that people consume an appropriate amount and to crack down on fake products. Traditional methods for detecting ascorbic acid, such as spectrophotometry[5],[6], electrochemistry[7], and chromatography[8],[9], are effective but often involve complex sampling processes and expensive testing equipment, making them less suitable for rapid and real-time analysis. Consequently, there is a growing demand for low-cost, fast, and accurate detection techniques, which has driven the rapid development of various sensors, including electrochemical, biochemical, and optical sensors, providing more affordable and effective solutions for food and drugs testing[10],[11].

Fiber-based sensors have extraordinary value and potential in food quality inspection, drug analysis, reaction kinetic monitoring, and biochemical detection fields[12],[13]. Wandermur et al. have proposed a novel and rapid-response plastic optical fiber (POF) biosensor for detecting Escherichia coli[14]. However, POFs suffered from significant light loss, poor high-temperature resistance, relatively lower sensitivity, and noticeable flaws, making them less suitable for applications requiring high-accuracy detection in harsh environments. Silica fiber sensors have also made significant progress in analysis[15]. While they demonstrate impressive performance in the near-infrared wavelength range below 2 μm, their transmittance and spectral range in the mid-infrared range above 2 μm is limited[16]. However, the basic vibration region of most compounds is concentrated in the mid-infrared region, and each molecule has its unique fingerprint region, which is why mid-infrared fiber optic sensors based on fiber evanescent wave sensing (FEWS) are particularly outstanding in the field of qualitative analysis of substances[17],[18]. In contrast, silver halide (AgCl) fibers demonstrate excellent transmission capabilities in the 4 μm to 16 μm wavelength range, effectively overcoming the limited transparency of silica fibers[19]. Recently, Zhou et al. validated the feasibility of in-situ identification of volatile compounds released by grapes using silver halide fibers, further demonstrating the enormous potential of fiber evanescent wave spectroscopy (FEWS) for qualitative analysis of substances[20]. However, silver halide fiber has poor optical stability, poor chemical resistance and high manufacturing cost, which limits its large-

This work is financially supported by the National Natural Science Foundation of China (61975156, U2241236) and the Open Projects Foundation (No. SKLD2202) of the State Key Laboratory of Optical Fiber and Cable Manufacture Technology (YOFC). *(Corresponding author: Yinsheng Xu).*

Tianxiang You, Yongkun Zhao, Haizheng Tao and Yinsheng Xu are with the State Key Laboratory of Silicate Materials for Architectures, Wuhan University of Technology, Wuhan 430070, China (e-mail: 15570398645@163.com; 15938312175@163.com; thz@whut.edu.cn; xuyinsheng@whut.edu.cn).

Yantao Xu and Haitao Guo are with the State Key Laboratory of Transient Optics and Photonics, Xi'an Institute of Optics and Precision Mechanics, Chinese Academy of Sciences (CAS), Xi'an, Shaanxi 710119, China (e-mail: xuyinsheng@whut.edu.cn; guoht_001@opt.ac.cn).

Jihong Zhu is the State Key Laboratory of Optical Fiber and Cable Manufacture Technology, Yangtze Optical Fibre and Cable Joint Stock Limited Company (YOFC), Wuhan 430073, China (e-mail: zhujihong@yofc.com).

Xianghua Zhang is with the Institut Des Sciences Chimiques de Rennes UMR 6226, CNRS, Université de Rennes 1, Rennes 35042, France (e-mail: xzhang@univ-rennes1.fr).

scale application[21],[22].

FEWS sensors based on chalcogenide fibers extend the detection signal range to the infrared region[23],[24]. Infrared light is absorbed by specific chemical bonds at characteristic frequencies, resulting in absorption peaks in the infrared spectrum[25]. This approach not only enables the detection of chemical substances and their concentrations in the sample but also facilitates the analysis of changes in biological tissues and tracking of chemical or biochemical reactions, as shown in **Fig. 1**. Chalcogenide fibers, which not only possess an exceptionally wide transmission range of 400 nm to 12 μm, covering the visible, near-infrared, and mid-infrared regions, but also exhibit excellent water and corrosion resistance[25],[26]. This allows them to directly immerse into the sample to record the information of the vanishing waves without causing any damage. The sensors do not need direct contact with the original test solution, only requiring a small sample volume (0.2 ml) to analyze the substance accurately. Additionally, glass-state optical fibers exhibit excellent chemical stability, thus alleviating concerns about potential contamination from harmful elements such as As[27],[28]. Furthermore, sulfide fibers are cost-effective, making them highly promising in sensing.

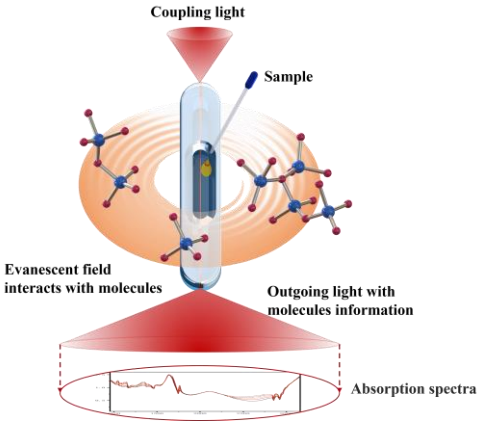

Fig. 1. Principle of infrared fiber evanescent wave sensing. Infrared light enters the fiber sensor and generates evanescent wave during propagation in the fiber. The evanescent wave of a specific wavelength resonates with the molecular groups of the analyte, producing a characteristic absorption spectrum carrying molecule information.

This work commences by synthesizing highly pure As_2S_3 glass and subsequently utilizing a fiber drawing tower to draw the glass into As_2S_3 fibers. Following a theoretical investigation using COMSOL software to examine the impact of waist diameter and bending on the sensor performance, a systematic fabrication process was employed to create four different structure fiber sensors, which were subsequently compared in terms of their sensing capabilities. Ultimately, the fiber with a waist diameter of 50 μm, a waist length of 30 mm, and a single bend was selected due to its outstanding sensing performance. This fiber structure was then employed to construct an evanescent wave sensor to precisely detect ascorbic acid in food and drugs. The sensor enables not only quantitative analysis but also addresses the issue of fake ascorbic acid products.

II. Material and Methods

A. Preparation of As_2S_3

High-purity (99.999%) As and S raw materials were used to synthesize purified As_2S_3 glass rods through melt-quenching. The glass rods were crushed and placed in a distillation tube in an Ar gas-protected glovebox. High-purity magnesium chips (250 ppm wt) and $TeCl_4$ were added as chemical scavengers. The distillation tube was then evacuated and sealed with a hydrogen-oxygen flame. The specific glass rod preparation process has been described in detail in the references[29]-[32]. Finally, a high-purity glass preform with a diameter of 15 mm and a length of 110 mm was obtained. The As_2S_3 glass sample was cut into 1.5 mm thick slices using a wire saw and then polished. Fourier Transform Infrared Spectroscopy (FTIR) (INVENIO S, Bruker, GE) was used to measure the optical transmission in the 2.5 to 25 μm range at room temperature. Finally, a high-precision fiber drawing tower (SGC, Customized) was used to draw the As_2S_3 glass rod into a 400 μm diameter optical fiber, and the fiber losses were calculated using the cutoff method[33].

B. Structure optimization and packaging of optical fiber

The tapered fibers were prepared using a homemade tapering setup consisting of two Linear Translation Stages (Thorlabs, NRT170), an aluminum heater, and an electron microscope. A 50 mm long fiber was fixed on each end of the Linear Translation Stage. The fiber was heated in the middle using the aluminum heater, slowly raising the temperature to the softening temperature of the fiber. Under the electron microscope, the fiber was observed to bend slightly, and the displacement stages were controlled by a custom program to control the fiber diameter and waist length precisely.

Four tapered fibers were fabricated using the tapering setup, with different waist diameters (d_w) and waist lengths (l_w). Specifically, one fiber had d_w = 75 μm and l_w = 10 mm, another had d_w = 75 μm and l_w = 30 mm, and two fibers had d_w = 50 μm and l_w = 30 mm. Among the fibers with d_w = 50 μm and l_w = 30 mm, one was manually coiled around a 4 mm diameter heating rod after being heated to its softening temperature. Finally, the four types of structured fibers were encapsulated in a 3D-printed liquid cell made of polylactic acid.

C. Construction of sensing device

Fig. 2 illustrates the fiber-enhanced evanescent wave spectroscopy (FEWS) experimental setup. Due to the large diameter and parallel nature of the beam output from the spectrometer, it cannot be efficiently coupled into the 400 μm cross-section of the fiber. Therefore, a plane mirror and an off-axis parabolic mirror were used for the first focusing of the beam, followed by a ZnSe lens for secondary focusing. This configuration allowed effective coupling of the focused light into the fiber sensor. The end face of the fiber was cut with a

blade to reduce coupling losses further. After passing through the liquid cell containing the target substance, the infrared light emitted carried absorption information and was collected by a Mercury Cadmium Telluride (MCT) detector. Finally, the signal was amplified and transmitted to a computer for analysis to obtain the absorbance spectrum of the sensor.

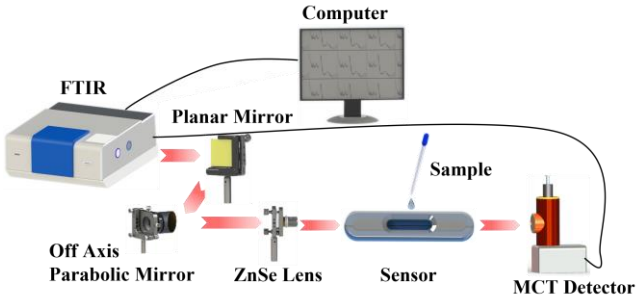

Fig. 2. Optical path of evanescent wave sensing experiment.

D. Preparation of liquid samples

Pure (99.99%) ascorbic acid powder was dissolved in water to prepare solutions with 5, 8, 11, 14, 17, 20, 30, 60, 90, 120, and 150 (mg/ml) concentrations, respectively. Two fruit juices rich in ascorbic acid, namely prickly pear juice, and sea buckthorn juice, along with three solid ascorbic acid products, Tongchen vitamin C effervescent tablets, Kangenbei vitamin C chewable tablets, and vitamin C tablets, were tested. The three tablets were ground into powder and dissolved in water for measurement.

III. Results and Discussion

A. Characterization of As_2S_3 fiber

Fig. 3 shows the loss of the As_2S_3 fiber in the range of 2 to 6.8 µm, with the lowest loss of 1.99 dB/m at 4.8 µm. As shown in the figure, some impurity peaks in the fiber, such as O-H (2.8 µm), H-S (3.1 µm, 3.6 µm, 4 µm), and H-O-H (6.3 µm), can be observed[18],[34]-[36].

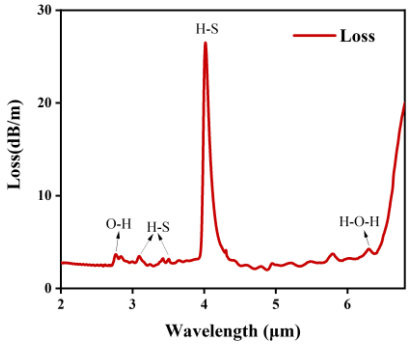

Fig. 3. Loss spectrum of As_2S_3 fiber in the 2-6.8 µm range.

A fiber cross-section was cut using an ultra-thin blade for scanning electron microscopy (SEM) analysis, as shown in **Fig. 4(a)**. The SEM image of the fiber cross-section reveals a smooth end face, which is essential for the effective coupling of the incident light and the fiber to meet the detection requirements. Additionally, the fiber diameter was 395 µm, with a tiny deviation from the designed fiber diameter. **Fig. 4(b-c)** show the Energy-Dispersive X-ray Spectroscopy (EDS) mapping results. The results indicate that the essential components of As and S are uniformly distributed within the fiber, with concentrations closely aligned with the design. The actual concentration of As is 59.7%, while that of S is 40.3%, with a deviation of no more than 0.3%.

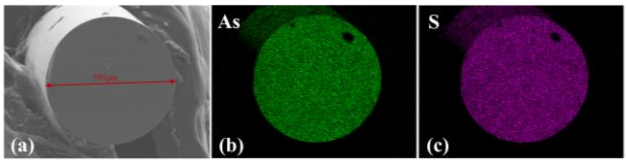

Fig. 4. (a) SEM image of As_2S_3 fiber end. (b-c) Element distribution of As and S at the fiber end.

B. Simulation of fiber with different structures

The penetration depth (d_p) of the evanescent wave determines the strength of interaction between the evanescent wave field and the analyte, as well as the performance of the sensor. The penetration depth is closely related to the wavelength and incident angle of the incident light, as well as the refractive indices of the fiber and the external medium, and is described by the following equation,

$$d_p = \frac{\lambda_i}{2\pi\sqrt{n_1^2 \sin^2 \theta_i - n_2^2}} \quad (1)$$

where λ_i and θ_i are the wavelength and incident angle of the incident light, and n_1 and n_2 are the refractive indices of the fiber and external medium, respectively. From this equation, we can see that changing the incident angle θ_i is an effective and feasible way to increase the penetration depth of the evanescent wave. Due to the good thermal stability of the As_2S_3 glass, it is feasible to enhance the sensing performance by tapering and bending them through controlled heating, thus reducing θ_i[37].

To further investigate the effects of reducing fiber diameter and bending on the evanescent waves, the evanescent wave intensity distribution in fibers with different diameters and curved configurations was simulated using the COMSOL Multiphysics software. As shown in **Fig. 5**, the evanescent wave intensity increases with the fiber diameter decrease, while the intensity is significantly enhanced in curved fibers. We assumed ideal conditions in this simulation without considering fiber losses and absorption. The core refractive index (n_1) was set to 2.41, corresponding to the refractive index of As_2S_3 glass, and the refractive index of the external environment (n_2) was set to 1.33. The incident wavelength was chosen as 5.69 µm, aligning with the characteristic vibrational absorption peak (1760 cm^{-1}) of the C=O bond in ascorbic acid. **Fig. 5(a)** displays the intensity distribution of the fundamental mode on the cross-section of straight fibers with diameters of 20 µm, 25 µm, and 30 µm, as well as their corresponding curved fibers. It is evident that in straight fibers, the intensity distribution of the fundamental mode shows a Gaussian bean distribution. However, the intensity distribution of the fundamental mode in the bent fiber shifts towards the outer side of the bend. **Fig. 5(b)** illustrates the relationship between the intensity of the fundamental mode and the distance from

the center of the fiber. It can be observed that the intensity decreases as the distance from the center increases. Interestingly, there is still a certain level of light beyond the boundary of the fiber. To facilitate the investigation of evanescent waves, the fundamental mode that extends beyond the fiber boundary was considered as the intensity of the evanescent waves for analysis purposes. A smaller fiber diameter in straight fibers corresponds to higher evanescent wave intensity and greater penetration depth. Comparing the evanescent wave intensities of straight fibers with the same diameter to those of curved fibers, it can be concluded that curved fibers exhibit significantly increased evanescent wave intensity and penetration depth. This lays a theoretical foundation for subsequent sensing experiments.

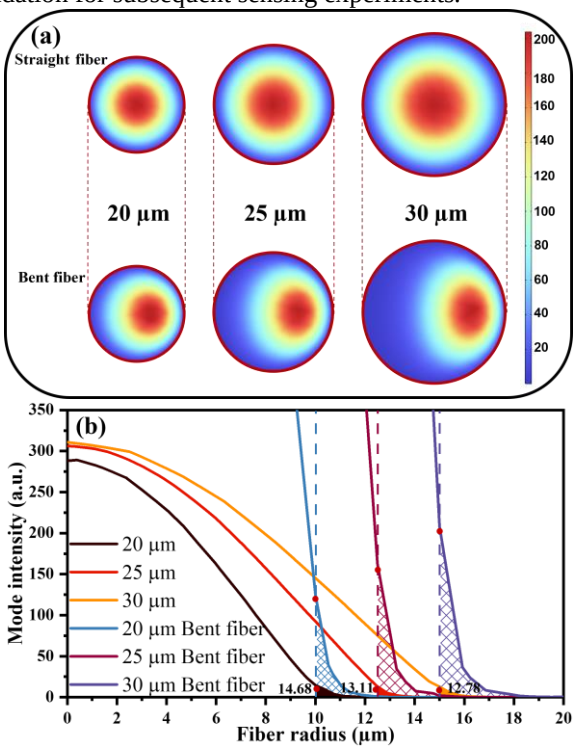

Fig. 5. (a) Fundamental mode strength distribution of straight and bent fiber with different diameters, 20, 25, and 30 μm. (b) the relationship between the fundamental mode strength and the distance from the center of the fiber. The shadow areas represent the field intensity of the evanescent wave.

C. Sensing properties of different fiber structures

The simulation results show that the sensing performance of fiber can be enhanced by optimizing the fiber structure by reducing the fiber radius and bending the fiber waist region. Hence, four fiber structures are proposed to increase the penetration depth of the evanescent wave. The parameters of the sensors are I: l_w=10 mm, d_w=75 μm, II: l_w=30 mm, d_w=75 μm, III: l_w=30 mm, d_w=50 μm, IV: l_w=30 mm, d_w=50 μm, and 1 circle (diameter: 4 mm), as shown in the inset of **Fig. 6 (I-IV)**. **Fig. 6(a-d)** shows the sensing results of the four sensors when detecting 30, 60, 90, 120, and 150 mg/ml ascorbic acid solutions. This detection is based on monitoring the C=C stretching vibration band of ascorbic acid at 1690 cm^{-1} and the C=O stretching vibration band at 1760 cm^{-1} as the basis for evaluating its sensing performance. Fig. 6 shows that regardless of the fiber structure, the intensity of the absorption peak increases with the increasing concentration of ascorbic acid. Under the same concentration of ascorbic acid solution, a comparison between **Fig. 6(a)** and **6(b)** reveals that the absorption peak intensity increases with the increasing waist length for the same waist diameter. Comparing **Fig. 6(b)** and **6(c)**, it can be seen that the absorption peak intensity increased by reducing the waist diameter for the same waist length. Furthermore, comparing **Fig. 6(c)** and **6(d)**, it is evident that for the same waist diameter and length, the absorption peak intensity of the bent fiber is higher than that of the unbent fiber.

Fig. 7(a) depicts the fitting results of the integrated area of the absorption peaks against the solution concentration, revealing a linear relationship between the two variables. The fitting line can be considered as the sensitivity of the fiber sensor. In **Fig. 7(b)**, the sensitivities of the four sensors are found to be 0.0708, 0.0978, 0.11, and 0.1257 (a.u./(mg·ml^{-1})), respectively. The LoD (C_{min}) was calculated using the following equation[38],

$$C_{\min} = \frac{3S_R}{S} \quad (2)$$

where S_R is the standard deviation of 10 tests of the absorbance of water, and S is the sensitivity. The calculated LoDs are as follows: 2.89, 1.78, 1.54, and 0.92 mg/ml, as shown in **Fig. 7(c)**. It is evident that as the fiber is continuously optimized, there is a gradual decrease in the LoD and an increase in sensitivity. This further underscores the importance of increasing the length of the waist region, reducing the diameter of the waist region, and bending the sensing region to enhance the sensitivity and lowering the LoD of the sensor. Through the above analysis, it can be inferred that the tapered ring fiber (type IV) exhibits optimal sensing performance. By increasing the length of the waist region, the interaction between the fiber and the analyte is enhanced. Furthermore, reducing the fiber diameter and bending the fiber contribute to shrinking θ_i and increasing the penetration depth d_p of the evanescent wave. These methods are beneficial to improving the sensing performance of the fiber sensor.

D. Testing experiment of ascorbic acid products

Because the tapered ring sensor (type IV) has the best sensing performance, this special fiber structure was chosen to manufacture the sensor, which enables the precise detection of ascorbic acid in ascorbic acid products. The newly developed sensor was initially tested using a low-concentration ascorbic acid solution, as shown in **Figure 8(a)**. It can be observed that even for low-concentration ascorbic acid solutions, there is a clear absorption peak due to the excellent sensing performance of the sensor. Sensitivity was obtained by fitting the integrated area of the absorption peak as the concentration increased. Subsequently, five different products containing ascorbic acid were tested, and their full spectra are shown in **Figure 8(b)**. Significant absorption peaks at 1690 cm^{-1} and 1760 cm^{-1} for

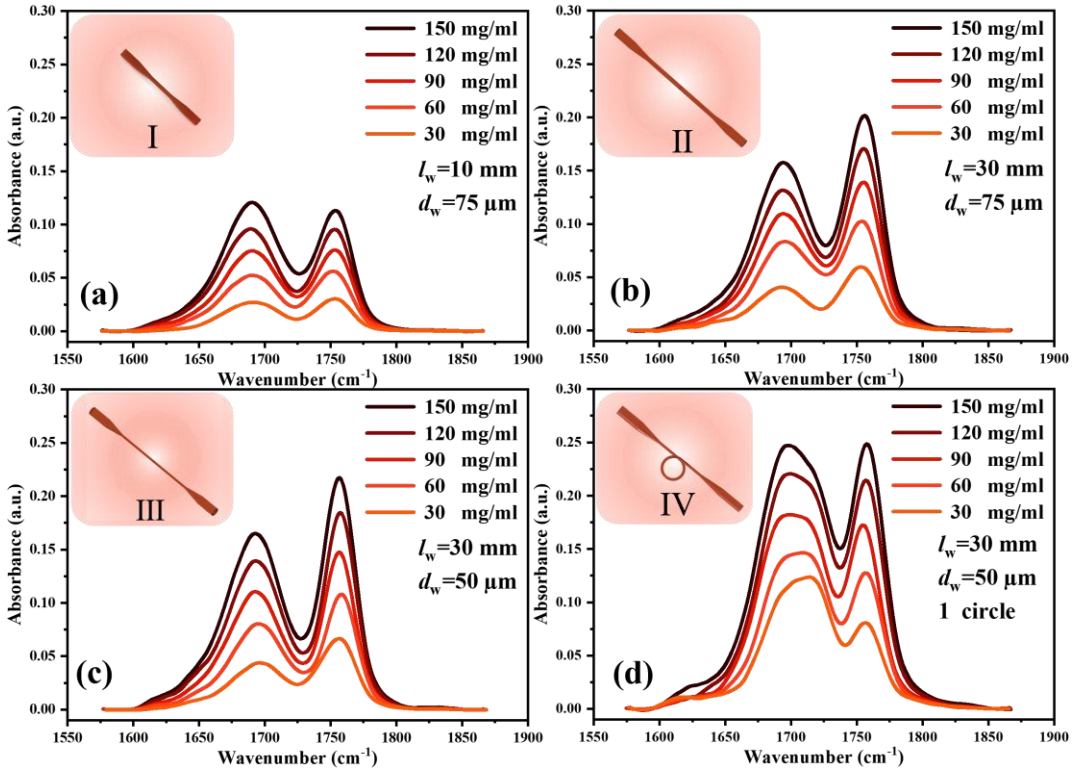

Fig. 6. Comparison of sensor performance. (a-d) Results of ascorbic acid solution detection by optical fiber sensors of different structures. Insets are the schematic of different types of sensors (I-IV).

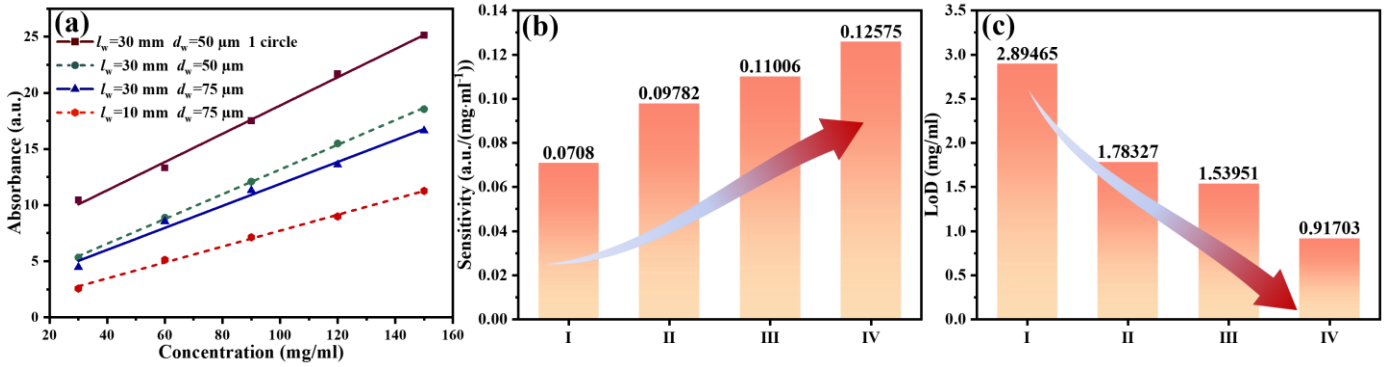

Fig. 7. Sensing performance of different sensors. (a) Sensitivity fitting curves of different sensors. (b) Sensitivity comparison of different sensors. (c) Comparison of the LoD of different sensors

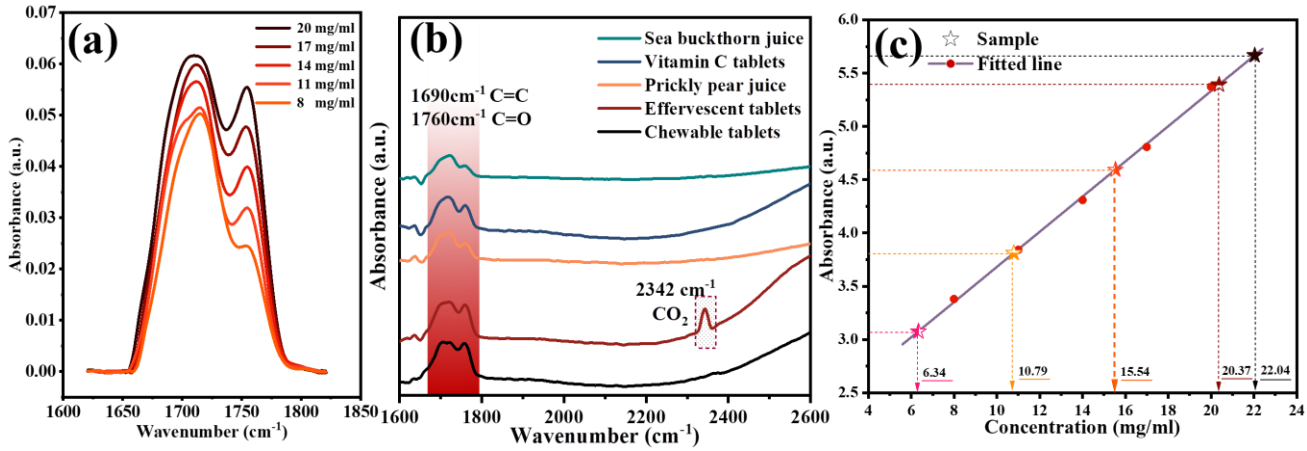

Fig. 8. Testing of ascorbic acid products by Type IV sensor. (a) Sensing results of low concentration ascorbic acid solution. (b) evanescent wave absorption spectra of five ascorbic acid products with characteristic peaks of carbon dioxide and ascorbic acid. (c) Measurement of ascorbic acid content in ascorbic acid products using fitted sensitivity curves.

all five products can be seen, indicating the presence of ascorbic acid. In addition, other fingerprint regions also showed clear absorption peaks. For example, there was a clear CO_2 absorption peak at 2342 cm^{-1} due to the release of a large amount of CO_2 when effervescent tablets dissolved in water. The sensitivity fitting curve obtained from testing low-concentration ascorbic acid solutions can be used as a standard to quantitatively analyze the concentration of ascorbic acid in these five products, as shown in **Figure 8(c)**. As shown in **Table 1**, the measured ascorbic acid content is very close to the nominal composition of the five products, with a maximum error of not exceeding 0.93 mg/ml.

TABLE I

MEASURED ASCORBIC ACID CONCENTRATION AND NOMINAL CONCENTRATION IN PRODUCTS

Sample	Measured content (mg/ml)	Nominal content (mg/ml)	Δ (mg/ml)
Chewable tablets	20.37	21.3	0.93
Effervescent tablets	22.04	22.5	0.46
Vitamin C tablets	10.79	10	0.79
Prickly pear juice	15.54	15	0.54
Sea buckthorn juice	6.34	6.15	0.19

IV. CONCLUSION

An infrared evanescent wave sensor for detecting ascorbic acid in food and drugs was developed using As_2S_3 infrared fiber. Through COMSOL software simulations, it was determined that decreasing the waist diameter and bending the fiber can enhance the evanescent wave intensity. The results show that the sensor with l_w=30 mm, d_w=50 μm, and 1 circle (diameter: 4 mm) has the best sensing performance. The characteristic absorption peaks at 1690 cm-1 and 1760 cm-1 can be identified for the ascorbic acid. The sensor exhibited a maximum sensitivity of 0.1257 (a.u./(mg·ml^{-1})) and the limit of detection (LoD) of 0.917 mg/ml for the detection of ascorbic acid. By analyzing the absorptions spectra of the food and drugs, the characteristic peaks of carbon dioxide and ascorbic acid can be identified. The qualitative and quantitative analysis with high accuracy for the food and drugs indicated that this fiber sensor can find applications in food and drugs quality monitoring.

REFERENCES

[1] J. Reang, P. C. Sharma, V. K. Thakur, and J. Majeed, "Understanding the Therapeutic Potential of Ascorbic Acid in the Battle to Overcome Cancer," *Biomolecules*, vol. 11, no. 8, pp. 1130, Jul. 2021.

[2] G. N. Y. Van Gorkom, E. L. Lookermans, C. H. M. J. Van Elssen, and G. M. J. Bos, "The Effect of Vitamin C (Ascorbic Acid) in the Treatment of Patients with Cancer: A Systematic Review," *Nutrients*, vol. 11, no. 5, pp. 977, Apr. 2019.

[3] M. Berretta *et al.*, "Multiple Effects of Ascorbic Acid against Chronic Diseases: Updated Evidence from Preclinical and Clinical Studies," *Antioxidants*, vol. 9, no. 12, pp. 1182, Nov. 2020.

[4] X. Yin *et al.*, "Chemical stability of ascorbic acid integrated into commercial products: A review on bioactivity and delivery technology," *Antioxidants*, vol. 11, no. 1, pp. 153, Jan. 2022.

[5] K. Kunpatee, S. Traipop, O. Chailapakul, and S. Chuanuwatanakul, "Simultaneous determination of ascorbic acid, dopamine, and uric acid using graphene quantum dots/ionic liquid modified screen-printed carbon electrode," *Sensors Actuators B: Chem.*, vol. 314, pp. 128059, Jul. 2020.

[6] I. S. A. Porto, J. H. Santos Neto, L. O. Dos Santos, A. A. Gomes, and S. L. C. Ferreira, "Determination of ascorbic acid in natural fruit juices using digital image colorimetry," *Microchem. J.*, vol. 149, pp. 104031, Sept. 2019.

[7] A. M. Pisoschi, A. Pop, A. I. Serban, and C. Fafaneata, "Electrochemical methods for ascorbic acid determination," *Electrochim. Acta*, vol. 121, pp. 443-460, Mar. 2014.

[8] L. Chen, W. Wang, J. Zhang, H. Cui, D. Ni, and H. Jiang, "Dual effects of ascorbic acid on the stability of EGCG by the oxidation product dehydroascorbic acid promoting the oxidation and inhibiting the hydrolysis pathway," *Food Chem.*, vol. 337, pp. 127639, Feb. 2021.

[9] L. V. De Faria *et al.*, "Direct analysis of ascorbic acid in food beverage samples by flow injection analysis using reduced graphene oxide sensor," *Food Chem.*, vol. 319, pp. 126509, Jul. 2020.

[10] S. Zhou, C. Liu, J. Lin, Z. Zhu, B. Hu, and L. Wu, "Towards Development of Molecularly Imprinted Electrochemical Sensors for Food and Drug Safety: Progress and Trends," *Biosensors*, vol. 12, no. 6, pp. 369, May. 2022.

[11] C. Dincer *et al.*, "Disposable Sensors in Diagnostics, Food, and Environmental Monitoring," *Adv. Mater.*, vol. 31, no. 30, pp. 1806739, Jul. 2019.

[12] T.-C. Liang, H.-S. Huang, and M.-H. Chuang, "Study on fiber grating sensors for concentration measurement of cottonseed oil adulteration in pure olive oil," *Microelectron. Eng.*, vol. 148, pp. 21-24, Aug. 2015.

[13] M. A. Butt, G. S. Voronkov, E. P. Grakhova, R. V. Kutluyarov, N. L. Kazanskiy, and S. N. Khonina, "Environmental monitoring: A comprehensive review on optical waveguide and fiber-based sensors," *Biosensors*, vol. 12, no. 11, pp. 1038, Nov. 2022.

[14] G. Wandermur *et al.*, "Plastic optical fiber-based biosensor platform for rapid cell detection," *Biosens. Bioelectron.*, vol. 54, pp. 661-666, Apr. 2014.

[15] Z. Li, Z. Wang, Y. Qi, W. Jin, and W. Ren, "Improved evanescent-wave quartz-enhanced photoacoustic CO sensor using an optical fiber taper," *Sensors Actuators B: Chem.*, vol. 248, pp. 1023-1028, Sept. 2017.

[16] G. Menduni *et al.*, "Fiber-Coupled Quartz-Enhanced Photoacoustic Spectroscopy System for Methane and Ethane Monitoring in the Near-Infrared Spectral Range," *Molecules*, vol. 25, no. 23, pp. 5607, Nov. 2020.

[17] M. Wang *et al.*, "Effect of the geometries of Ge-Sb-Se chalcogenide glass tapered fiber on the sensitivity of evanescent wave sensors," *J. Lightwave. Technol.*, vol. 39, no. 14, pp. 4828-4836, Jul. 2021.

[18] A. P. Velmuzhov, V. S. Shiryaev, M. V. Sukhanov, T. V. Kotereva, B. S. Stepanov, and G. E. Snopatin, "Mid-IR fiber-optic sensors based on especially pure $Ge_{20}Se_{80}$ and $Ga_{10}Ge_{15}Te_{73}I_2$ glasses," *J. Non-Cryst. Solids*, vol. 579, pp. 121374, Mar. 2022.

[19] A. Yuzhakova, D. Salimgareev, A. Lvov, A. Korsakov, and L. Zhukova, "Infrared fibers manufacture from single crystals of the AgBr-AgI system," *Opt. Mater.*, vol. 131, pp. 112687, Sept. 2022.

[20] Y. Zhou *et al.*, "In situ detection of fruit spoilage based on volatile compounds using the mid-infrared fiber-optic evanescent wave spectroscopy," *Front. Plant Sci.*, vol. 13, pp. 991883, Oct. 2022.

[21] A. Yuzhakova, D. Salimgareev, A. Lvov, A. Korsakov, and L. Zhukova, "Numerical simulation and manufacturing of infrared photonic-crystal fibers based on the AgBr–AgI system crystals for the 2–25 μm," *Opt. Mater.*, vol. 121, pp. 111642, Nov. 2021.

[22] J. Wei *et al.*, "Bioinspired cellulose - integrated MXene - based hydrogels for multifunctional sensing and electromagnetic interference shielding," *Interdiscip. Mater.*, vol. 1, no. 4, pp. 495-506, Oct. 2022.

[23] L. Jiao, N. Zhong, X. Zhao, S. Ma, X. Fu, and D. Dong, "Recent advances in fiber-optic evanescent wave sensors for monitoring organic and inorganic pollutants in water," *TrAC, Trends Anal. Chem.*, vol. 127, pp. 115892, Jun. 2020.

[24] Y. Yang *et al.*, "Mid-infrared evanescent wave sensor based on side-polished chalcogenide fiber," *Ceram. Int.*, vol. 49, no. 1, pp. 1291-1297, Jan. 2023.

[25] Y. Raichlin and A. Katzir, "Fiber-optic evanescent wave spectroscopy in the middle infrared," *Appl. Spectrosc.*, vol. 62, no. 2, pp. 55A-72A, Feb. 2008.

[26] A. P. Velmuzhov *et al.*, "Fiber sensor on the basis of $Ge_{26}As_{17}Se_{25}Te_{32}$ glass for FEWS analysis," *Opt. Mater.*, vol. 75, pp. 525-532, Jan. 2018.

[27] P. Lucas, A. A. Wilhelm, M. Videa, C. Boussard-Plédel, and B. Bureau, "Chemical stability of chalcogenide infrared glass fibers," *Corros. Sci.*, vol. 50, no. 7, pp. 2047-2052, Jul. 2008.

[28] A. A. Wilhelm, P. Lucas, D. L. DeRosa, and M. R. Riley, "Biocompatibility of Te–As–Se glass fibers for cell-based bio-optic infrared sensors," *J. Mater. Res.*, vol. 22, no. 4, pp. 1098-1104, Apr. 2007.
[29] V. S. Shiryaev, M. F. Churbanov, G. E. Snopatin, and F. Chenard, "Preparation of low-loss core-clad As-Se glass fibers," *Opt. Mater.*, vol. 48, pp. 222-225, Oct. 2015.
[30] T. Kang-Zhen *et al.*, "Ge-As-S chalcogenide glass fiber with high laser damage threshold and mid-infrared supercontinuum generation," *Acta Phys. Sin.*, vol. 70, no. 4, Feb. 2021.
[31] Q. Qi *et al.*, "A gas-liquid sensor functionalized with graphene-oxide on chalcogenide tapered fiber by chemical etching," *J. Lightwave. Technol.*, vol. 39, no. 21, pp. 6976-6984, Nov. 2021.
[32] V. S. Shiryaev *et al.*, "Core-clad terbium doped chalcogenide glass fiber with laser action at 5.38 μm," *J. Non-Cryst. Solids*, vol. 567, Sept. 2021.
[33] B. Zhang *et al.*, "Low Loss, high NA chalcogenide glass fibers for broadband mid-infrared supercontinuum generation," *J. Am. Ceram. Soc.*, vol. 98, no. 5, pp. 1389-1392, May. 2015.
[34] J. Wang *et al.*, "Se-H-free As_2Se_3 fiber and its spectral applications in the mid-infrared," *Opt. Express*, vol. 30, no. 13, pp. 24072, Jun. 2022.
[35] Z. Feng *et al.*, "Low-loss single-mode Ge–As–S–Se glass fiber and its supercontinuum generation for mid-infrared," *Opt. Commun.*, vol. 515, pp. 128189, Jul. 2022.
[36] M. F. Churbanov, I. V. Skripachev, G. E. Snopatin, L. A. Ketkova, and V. G. Plotnichenko, "The problems of optical loss reduction in arsenic sulfide glass IR fibers," *Opt. Mater.*, vol. 102, pp. 109812, Apr. 2020.
[37] H. Yang *et al.*, "Noninvasive and prospective diagnosis of coronary heart disease with urine using surface-enhanced Raman spectroscopy," *Analyst*, vol. 143, no. 10, pp. 2235-2242, Aug. 2018.
[38] Z. Li *et al.*, "Infrared evanescent wave sensing based on a $Ge_{10}As_{30}Se_{40}Te_{20}$ fiber for alcohol detection," *Sensors*, vol. 23, no. 10, pp. 4841, May. 2023.

Tianxiang You was born in China in 1998. Since 2021, he has been studying materials and Chemical Engineering at the School of Materials Science and Engineering, Wuhan University of Technology. He is mainly engaged in the research of infrared fiber sensor.

Yongkun Zhao was born in China in 1999. Since 2021, he has been studying materials and Chemical Engineering at the School of Materials Science and Engineering, Wuhan University of Technology. He is mainly engaged in the research of infrared fiber sensor.

Yantao Xu obtained his Ph.D. in Materials Science from the University of the Chinese Academy of Sciences in 2019. He is currently an Associate Researcher at the Xi'an Institute of Optics and Precision Mechanics, Chinese Academy of Sciences. His main research areas include infrared photon functional materials, special infrared glass, and fiber research.

Haitao Guo received his Ph.D. in Materials Science from Wuhan University of Technology in 2007. He is currently the Director of the Photon Functional Materials and Devices Laboratory at the Xi'an Institute of Optics and Precision Mechanics, Chinese Academy of Sciences. His research focuses on the preparation and spectral properties of infrared glasses, such as rare earth-doped sulfide and tellurite glasses, as well as the nonlinear and magneto-optical properties of infrared glasses.

Jihong Zhu is currently a Ph.D. candidate in Materials Science at Wuhan University of Technology. He is also the General Manager of Changfei Fiber Optic Cable Co., Ltd. His research mainly focuses on the design of fiber preforms, fiber optic product development, and the study of high-purity quartz materials.

Haizheng Tao received his Ph.D. in Materials Science from Wuhan University of Technology in 2004. He is currently a Researcher and Ph.D. Supervisor at the State Key Laboratory of Silicate Materials for Architectures. His main research interests include optoelectronic information and functional materials, infrared transmitting materials, as well as functional glass and film materials.

Xianghua Zhang obtained his Ph.D. in Solid State Chemistry from the University of Rennes in France in 1988. he is currently a Senior Researcher and Director at the National Center for Scientific Research in France. His primary research focus is on the development of infrared nanocomposite materials.

Yinsheng Xu obtained his Ph.D. in Materials Science and Engineering from East China University of Science and Technology in 2011. He is currently a Researcher at the State Key Laboratory of Silicate Materials for Architectures. His main research areas include infrared glass and fibers, as well as luminescent materials and devices.